INTERFACE

rsif.royalsocietypublishing.org

Research

Cite this article: Mortimer B, Soler A, Siviour CR, Zaera R, Vollrath F. 2016 Tuning the instrument: sonic properties in the spider's web. *J. R. Soc. Interface* **13**: 20160341. http://dx.doi.org/10.1098/rsif.2016.0341

Received: 1 May 2016
Accepted: 10 August 2016

Subject Category:
Life Sciences–Physics interface

Subject Areas:
biomaterials, biomechanics, biophysics

Keywords:
finite-element analysis, *Araneus diadematus*, vibration, waves, supercontraction

Author for correspondence:
B. Mortimer
e-mail: beth.mortimer88@gmail.com

Electronic supplementary material is available online at https://dx.doi.org/10.6084/m9.figshare.c.3457485.

THE ROYAL SOCIETY PUBLISHING

Tuning the instrument: sonic properties in the spider's web

B. Mortimer[1], A. Soler[3], C. R. Siviour[2], R. Zaera[3] and F. Vollrath[1]

[1]Department of Zoology, and [2]Department of Engineering Science, University of Oxford, Oxford, UK
[3]Department of Continuum Mechanics and Structural Analysis, Universidad Carlos III de Madrid, Madrid, Spain

BM, 0000-0002-7230-3647

Spider orb webs are multifunctional, acting to absorb prey impact energy and transmit vibratory information to the spider. This paper explores the links between silk material properties, propagation of vibrations within webs and the ability of the spider to control and balance web function. Combining experimental and modelling approaches, we contrast transverse and longitudinal wave propagation in the web. It emerged that both transverse and longitudinal wave amplitude in the web can be adjusted through changes in web tension and dragline silk stiffness, i.e. properties that can be controlled by the spider. In particular, we propose that dragline silk supercontraction may have evolved as a control mechanism for these multifunctional fibres. The various degrees of active influence on web engineering reveals the extraordinary ability of spiders to shape the physical properties of their self-made materials and architectures to affect biological functionality, balancing trade-offs between structural and sensory functions.

1. Introduction

Spider orb webs are two-dimensional snares that function to capture prey and transmit sensory information to the spider [1–3]. Orb webs contain five different silk materials (figure 1): a combination of major ampullate (or dragline) silk and minor ampullate silk for the converging radial threads, a combination of flagelliform and aggregate silk for the encircling capture spiral [4,5], and the cement of the anchor points and thread intersections [6]. Although dragline silk is known for its exceptional toughness and high tensile strength, the capture spiral is better known for its large strain elasticity and adhesive properties [7,8].

In addition to their role as structural elements, web silks are also able to act as signal lines by transmitting vibrations to the spider. In this way, specific structural threads provide information relevant for prey capture (and also courtship) [9–11]; and web vibrations can come not only from environmental sources such as wind [12], but also from biological sources such as prey, potential mates and even predators [13]. Importantly, spiders possess very sensitive vibration sensors on each that enable them to use this silk-linked information source [14,15].

The spider of this study, the garden cross spider *Araneus diadematus*, monitors radial thread vibration at the centre of the web. Orb web vibrations propagate as transverse, longitudinal and lateral waves [3] and the first two are studied in this paper. Transverse wave particle oscillation is perpendicular to the fibre axis and web plane, with speed being governed by string tension and mass per unit length [16]. Radial thread tension affects this kind of information flow, and tensions are closely monitored and controlled by spiders during web construction [17–19] with the animal potentially altering web tension in response to changes in environmental conditions and even prey presence [20,21]. Longitudinal wave particle oscillation, by contrast, is along the fibre axis and transmission speed is governed by material density and stiffness [16]. Here, the animal can control the modulus (stiffness) of the radial threads made from major ampullate silk during spinning and post-processing [22,23]. However, the modulus is also

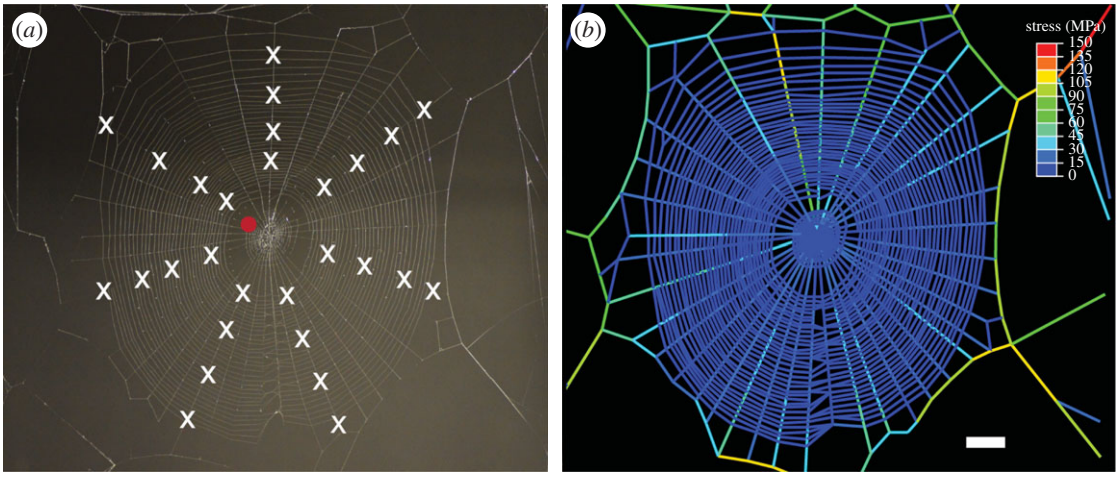

Figure 1. Modelling of *Araneus diadematus* webs. (*a*) Photograph of actual web 1. The vibration input signal was placed at different locations on the web (denoted by crosses) and the output was measured always at the same one location (circle). Converging radial and framing threads are made from major ampullate silk and the encircling capture spiral is made from flagelliform/aggregate silk. (*b*) Model of web 1, where colours/shades shows pre-stress levels in different parts of the web following equilibrium. White bar denotes 20 mm. (Online version in colour.)

affected by the phenomenon of supercontraction—a process whereby a slack silk fibre contracts up to 50% when exposed to water [24,25].

Experimental measurements of orb web vibration have shown that transverse waves tend to have the largest amplitude at the vibration source, while longitudinal waves are propagated with the least attenuation [3,26,27]. Although frequency dependence of amplitude spectra of different wave types is well documented [3,12,26,27], experimental data on the patterns of wave propagation through webs are lacking.

Mechanical modelling provides a valuable methodology to study the structural performance of orb webs in detail and has been deployed to uncover specific aspects of web behaviour under a variety of quasi-static [28–32] and dynamic [33–37] loading conditions. However, the potential of mechanical modelling for the study of wave propagation in webs has been largely unexploited. Here, a nonlinear dynamic finite-element analysis (FEA) model of *A. diadematus* orb webs was developed to include (i) a detailed simulation of the real architecture of the web, (ii) the material properties of the silk (here modelled as a linear elastic material, which is a relevant approximation for small amplitude vibration propagation), (iii) the pre-stress fields and (iv) the nonlinear aerodynamic drag forces.

These models allowed in-depth analysis of the transmission of sensory information along the silk threads by means of a finite duration wave pulse. The comparison of the models with experimental data from real webs allowed quantitative analysis of the link between silk material properties, elastic propagation of vibrations and the degree to which silk properties can be controlled and tuned. This in turn provided novel insights into the natural design of orb webs as multifunctional structures that have both mechanical and sensory functions. Control of web properties by the spider would suggest that evolution can exploit physical laws in order to achieve biological function.

2. Material and methods

2.1. Spiders and webs

Araneus diadematus spiders were collected in Oxford City and kept in laboratory conditions (approx. 20°C, 40% RH and a 16 L : 8 D cycle). Spiders ($N = 3$) had to make at least two webs before a sample web was used for any measurements. All spiders were handled according to local laboratory risk assessments/institutional ethical guidelines and do not currently fall under regulation by UK or EU legislation. Webs ($N = 3$) were photographed and traced digitally to create a model version of the exact web architecture, which incorporates the geometries of the capture spiral, radial threads and mooring threads, which differ between the webs from each individual. Distances of the experimental points relative to the laser position during vibrometry experiments were calculated using ImageJ (National Instruments), repeating the measurements three times. The density of silk was assumed to be 1325 kg m^{-3} [38].

2.2. Vibrometry

A small pulse from a solenoid (3 ms square wave) was placed orthogonally onto web radial threads. The solenoid input was moved about the web, positioned on seven or eight different radials, each with three or four locations of varying distances from the hub (e.g. see figure 1). Web vibration (without the spider) was measured using a laser Doppler vibrometer (Polytec PSV-400), where the laser was focused orthogonal to the web, allowing the measurement of transverse waves only. The laser focus point remained stationary—near the hub in a location where usually one of the spiders' legs would touch (figure 1). The reference movement of the solenoid was measured for each solenoid position using a PDV-100 vibrometer (Polytec). Both vibrometers were triggered from the voltage input into the solenoid. For each solenoid position, five velocity–time datasets were gathered at the hub, together with one reference velocity–time dataset. The reference start times and maximum displacement amplitudes were averaged across all the data for each web to generate an input time–displacement profile (average displacement of 171 ± 15 µm, $N = 83$). This displacement was four times bigger than transverse displacements measured for real prey struggling in the web [12]; smaller displacements, however, would have provided signal to noise ratios impractical for this set-up. All data were analysed using a custom written Matlab code (more details in electronic supplementary material, Methods).

2.3. Modelling

The finite-element models were created using the commercial code ABAQUS/Explicit 6.14–2. The web architectures were transferred from photographs of real webs of *A. diadematus*, with only the hub

being simplified in the model (figure 1; electronic supplementary material, figure S1). Anchor threads were pinned at their boundaries to prevent displacements at the ending of the strands. More details on the model and material properties are given in the electronic supplementary material, Methods.

Owing to the low strain values reached in the web during the analysis (radial threads were always less than 1%), a linear elastic behaviour was used for this model. Aerodynamic drag forces were introduced following the methodology proposed in Zaera *et al*. [33]. Given the relevance of the stress level in the propagation speed of transverse waves, a pre-stress field was introduced in the webs. This tension field was applied as an initial step before a vibration input. The web was given time to equilibrate, where the model adjusted the pre-stress of the radial threads iteratively until it reached final pre-stress values that included a pre-stress gradient at least equal to those recorded for real webs [19].

Four analyses were carried out for each web architecture: reference pre-stress with and without capture spiral and stiff hub, double reference pre-stress and no pre-stress. The numerical simulation consisted of two steps: (i) the web was given time to reach mechanical equilibrium after imposing an initial pre-stress field, (ii) a radial node was vibrated using the averaged time-displacement profile from experimental measurement of the solenoid. Both excited (input) and control (output) points were placed at the positions selected for the experimental tests.

3. Results and discussion

The results and ensuing discussion are split into three sections. The first covers transverse waves and the role of pre-stress in the web, which utilizes both experimental and FEA modelling approaches. The second section compares longitudinal to transverse waves using FEA modelling data, comparing amplitude response and the role of silk modulus. The final section summarizes the links between silk material and sonic properties and the control mechanisms used by the spider to tune these properties to its advantage.

3.1. Transverse waves and pre-stress

Our FE models were created using different web architectures from three individual spiders as an input. Following the equilibrium of web tension, it emerged that pre-stress varied between radials within a web and also between webs, suggesting that a web architecture input can influence the resulting equilibrated pre-stress patterns between and within our model webs (figure 1; electronic supplementary material, figure S1). Previous studies support the assumption that spiders control web pre-stress during web building [18,19], but further experimental evidence is required to assess whether spiders can and do use web architecture to control web pre-stress through a combination of tensioning during web building and passive equilibrium of tensions within the mesh structure.

The models suggested that web architecture (arrangement of radial threads, capture spiral and mooring threads) can alter pre-stress within webs, which needs validating with further experimental evidence. Firstly, pre-stress was unevenly shared across different radials within a web according to their relationship with the surrounding mooring threads. As the differences in stress were small and within the elastic region (maximum pre-stress on a radial was 100 MPa), this pattern did not cause detectable differences in wave transmission in our experimental or modelling data. Secondly, when webs from different spiders were compared, some webs had larger variations in pre-stress values than others (electronic supplementary material, figure S1). For example, one web did not have a pre-stress gradient on a quarter of radials (electronic supplementary material, figure S1*d*), showing that in our models the web architecture input directly influenced the web's pre-tensioning output following the equilibrium of tensions within the mesh structure.

A small transverse displacement pulse from a solenoid was used to generate the vibration input for the experiments and the equivalent input was modelled in the simulations. Transverse waves were easily visualized following web impact (electronic supplementary material, Video S1). Figure 2 compares data from experiments and models, showing the displacement-time profiles of transverse waves as a response to the input-pulse being moved along a single radial thread. Table 1 compares other transverse wave features for all three webs. Included are data from FE models in which (i) webs had double the pre-stress of the literature values and (ii) webs contained no cross threads (neither the capture spiral nor cross threads at the hub), which removed the radial pre-stress gradient and the impedance differences at radial thread/capture spiral junctions.

Comparisons of the modelling and experimental data give information on differences in pre-stress and damping between the real and model webs. Pre-stress is very important for transverse wave propagation, which was shown by FE models with no pre-stress where there was no propagation of transverse waves following impact. This is because transverse waves can only propagate in fibres with finite tensions, as the wavespeed, C_T, is equal to $(T/\mu)^{1/2}$, where T is the tension and μ the mass per unit length. Estimates of pre-stress gradients along radial threads for the real webs were made from the transverse wavespeed values. Comparing the experimental transverse wavespeed to the three models (table 1), our data suggest that the webs used here had higher maximum tensions and higher tensioning gradients along radial threads than previously reported [19]. In fact, based on the relationship between transverse wavespeed (C_T), stress and density (stress $= {C_T}^2 \times$ density), our maximum transverse wavespeed data translated to maximum average (bulk) pre-stress values of 29, 46 and 40 MPa for points on each of the three experimentally measured webs. These maximum pre-stress points were positioned close to the web frame and pre-stress values remained within the elastic region of major ampullate silk.

Transverse waves also dampen, or attenuate, as the propagation distance along a radial increases. Results of damping calculations from experiments and models were in comparable ranges, but the models did not capture the higher damping seen in the experimental data (table 1). Decreases in maximum displacement amplitude may be caused by aerodynamic damping, internal damping or pulse amplitude spreading (a result of dispersion owing to the web architecture); the last of these does not absorb energy but spreads the pulse energy out across the web. Although aerodynamic damping and amplitude spreading were taken into account in our models, internal damping was not covered as the models used only purely elastic properties. Our results suggest that in real webs energy was dissipated through internal damping; even after a small amplitude impact, the high pre-stresses in the real webs made the viscoelastic silk dissipate energy. We note that only 13 out of 22 radials measured experimentally allowed a damping coefficient to be calculated, which can be explained in part by experimental

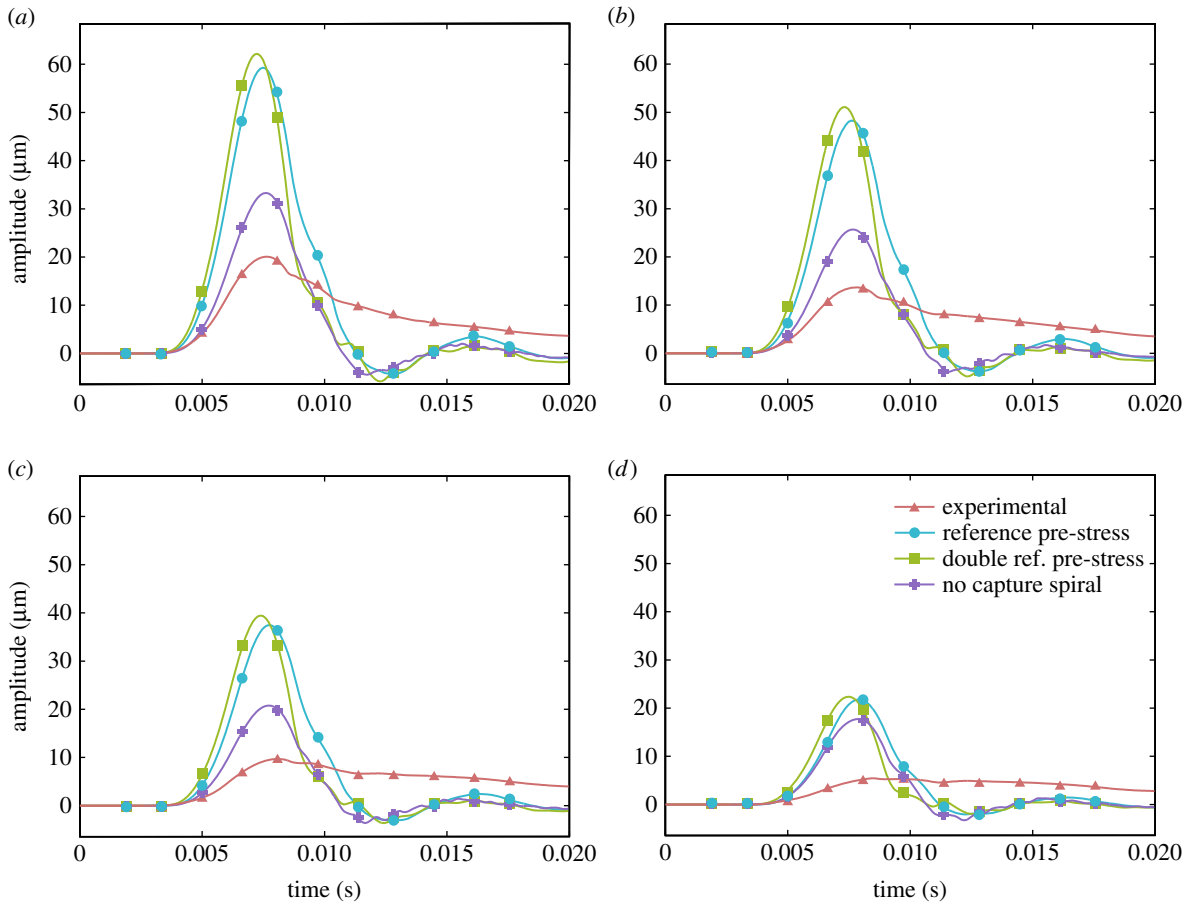

Figure 2. Propagation of transverse displacement over time, where the inputs were at distances of (*a*) 34 mm, (*b*) 47 mm, (*c*) 64 mm and (*d*) 95 mm from the output measurements on a single radial (web 1). Amplitudes are a proportion relative to the maximum displacement magnitude for each dataset. Red gives experimental data, blue gives model with pre-stress from literature, green gives model with double pre-stress and purple gives model with no capture spiral, where maximum input displacement was approximately 170 µm and damping was −1.68, −1.47, −1.53 and −0.64 dB cm^{-1}, respectively. (Online version in colour.)

variation (as each sample was measured in a separate experiment) and in part by the action of the stiff hub or frame cross threads. Furthermore, following the peak maximum, the difference in the shape of the experimental data in figure 2 can be explained by air drag [2]. Our models applied a displacement forward and backward, whereas the solenoid only provided a forward pulse and did not actively return the thread to its equilibrium location; air drag acting on the web during experiments reduces this return speed and thus increases the duration of the pulse.

In terms of absolute amplitude, the maximum displacement amplitudes in the models were higher than those measured experimentally (table 1). Although the amplitude of the transverse wave induced in the model was the same as the displacement amplitude of the solenoid, it is assumed that the experimental data were lower because of imperfect coupling between the solenoid and the web. These and other insights gained from the comparison of experimental data and interpretative modelling highlight the importance of combining the two techniques to develop a more comprehensive understanding of the range of parameters and variables that affect vibration transmission in the spiders' web.

Comparisons of the FE models revealed the functions of cross threads, including the capture spiral, for transverse wave propagation in the web. Firstly, without the capture spiral the pre-stresses in radial fibres were lower on average, which made the transverse wavespeed lower than the reference model, albeit with overlapping range (table 1). Secondly, the capture spiral influenced damping. Damping with increased distance followed the expected trend for the reference and double pre-stress models, whereas in the model without a capture spiral, for 16 out of 22 radials there was an increase in measured amplitude when the solenoid was placed near the outer end of a radial, near the bridging threads. At these positions, the transverse excitation displaced the bridging threads (as well as the radial thread) and so more elastic energy was imparted into the system.

Thirdly, regarding the capture spiral, maximum displacement amplitudes of transverse waves were larger for the reference model web with the capture spiral than for the model without spiral threads. This was unexpected as the capture spiral should reduce the amplitude of transverse waves [27], as seen in webs of *Nephila* species that have a stiff auxiliary spiral in addition to the much softer capture spiral [26]. Amplitudes would be expected to be lower with the capture spiral in our *Araneus* webs due to (i) impedance changes at junctions between the radial threads and capture spiral and (ii) through amplitude spreading of transverse waves as they move through the capture spiral to other radials (figure 3). We propose the reason for the higher amplitudes for the model with a capture spiral is possibly that we used a fixed excitation amplitude, so radial threads that are interconnected by the capture spiral will have a higher energy input. Additionally, pre-stress gradients can only be supported if the capture spiral is present, which could play a role: as the wave moves inward along a radial from a location of

Table 1. Experimental data versus model outputs for transverse waves, giving maximum and minimum speeds and damping, and highest and lowest maximum absolute displacements where *N* denotes number of samples. Some experimental data points for speed were not included if the variation was too high or if it was not possible to calculate a damping gradient across all radials (see the electronic supplementary material, Methods). (Online version in colour.)

web	experimental/ model	model treatment	*N*	max. speed ($m\ s^{-1}$)	min. speed ($m\ s^{-1}$)	*N*	highest max. displacement (μm)	lowest max. displacement (μm)	*N*	max. damping ($dB\ cm^{-1}$)	min. damping ($dB\ cm^{-1}$)
1	experimental		26	146.7	35.3	27	20.8	1.3	6	−2.75	−0.79
1	model	reference	27	74.6	32.5	27	60.5	17.4	7	−1.47	−0.76
1	model	double pre-stress	27	102.4	39.1	27	62.2	18.7	7	−1.53	−0.85
1	model	no capture spiral	27	67.8	32.5	27	33.3	7.6	2	−0.64	−0.51
2	experimental		28	185.5	31.0	31	32.4	1.0	4	−3.12	−1.76
2	model	reference	31	64.1	27.5	31	51.1	18.2	8	−1.13	−0.61
2	model	double pre-stress	31	86.5	30.6	31	59.2	20.7	8	−1.09	−0.59
2	model	no capture spiral	31	63.6	25.6	31	38.4	7.6	1		−0.42
3	experimental		23	173.0	46.8	27	21.7	2.1	3	−2.50	−0.86
3	model	reference	27	99.3	53.4	27	50.1	11.2	7	−1.45	−0.80
3	model	double pre-stress	27	131.6	69.2	27	58.1	12.8	7	−1.50	−0.86
3	model	no capture spiral	27	94.0	34.9	27	29.3	8.3	2	−1.00	−0.56

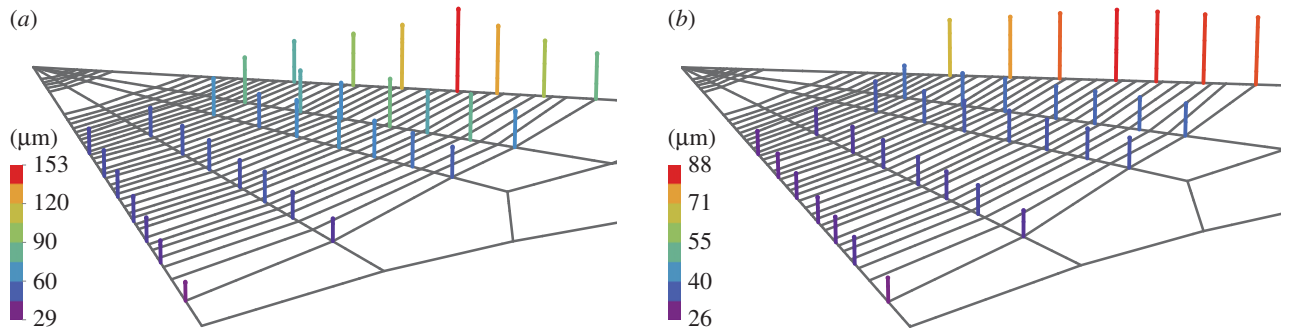

Figure 3. Amplitude spreading in a segment of the web for (*a*) transverse waves and (*b*) longitudinal waves where input was at a 60° angle (where 90° was orthogonal to web plane). Heights and colours of bars denote relative amplitude, where red/tallest bar is the maximum displacement for the panel (100%) and purple/short bar gives the lowest displacement for the panel. (Online version in colour.)

higher pre-stress to one of lower pre-stress, the amplitude will tend to increase. This appeared to have a greater effect on amplitude than impedance changes or amplitude spreading, meaning that webs with a capture spiral had higher output amplitudes because they had higher pre-stress gradients. The capture spiral therefore directly influences both pre-stress and damping of transverse waves, and this aspect of web architecture is directly under control by spiders during web building [1].

The model where pre-stress was doubled showed that the transverse wavespeeds measured were (as expected) significantly higher than those in the reference model. Damping was in a similar range to the reference model and maximum displacement amplitude was on average higher than the reference model, but with overlapping ranges (table 1). These data support the assertion [21] that a higher pre-stress increases the sensitivity of the web to vibrations; indeed, it has been shown that increasing web tension helps spiders detect smaller prey [20]. However, higher web pre-stress may have detrimental effects, for example decreased prey retention or lower damage tolerance as highly tensioned silk is more likely to yield [21].

Our models suggest that web architecture directly influences web pre-stress. This is an interesting observation deserving further experimental evidence. If used, adjusting web architecture would allow spiders to shape the trade-off between mechanical performance and vibration sensitivity, as web pre-stress is important for both. The property of supercontraction in major ampullate silk is a good candidate for controlling pre-stress in radial threads, as discussed in the following section.

3.2. Longitudinal waves and modulus

Longitudinal wave propagation in webs was investigated using the FE models. The models showed that longitudinal waves differ from transverse waves, as expected from the theory governing our models. The angle of input had a large effect on the amount of longitudinal energy being introduced (electronic supplementary material, figure S2). In reality, impact into the web is likely to be at velocities whose largest components are normal to the web surface; however, transverse impacts generate longitudinal waves that precede the transverse vibration [39]. Prey retained following impact will create vibrations that will be a mixture of both transverse and longitudinal waves [12,26], where the angle will alter the relative amplitudes of transverse and longitudinal components.

Our models provide insights into how transverse and longitudinal waves spread over the web after impact (figure 3). Impact was at a fixed location halfway along a radial thread. On radials adjacent to the impact, transverse wave amplitude was highest in the centre of the radial, but longitudinal waves were more consistent in their amplitude levels along radial length. This suggests that longitudinal waves leaked to other radials via both the stiff hub cross threads and the bridging threads, whereas transverse waves leaked also via the capture spiral. Comparing between radials, amplitudes were lower on radials further from impact for both transverse and longitudinal waves. In fact, the energy difference between the impacted and adjacent radial was 29% for transverse and 52% for longitudinal waves, with a further 19% and 9%, respectively, energy difference to the next radial. Transverse waves were therefore more dispersive as more energy was transferred between adjacent radials. Longitudinal waves were less dispersive as the waves must translate into transverse waves in the capture spiral to transfer energy, but not much energy was transferred as the amplitudes of longitudinal waves were small and tensions in the capture spiral were low. Therefore, longitudinal waves had more directional information in their absolute amplitudes, making them more useful for determining vibration source direction, which is supported with previous experimental data [3,26,27].

We investigated nonlinearity in the system by applying impacts of different displacement magnitudes into our model webs (figure 4). Given a transverse input, the maximum displacement amplitude of longitudinal waves was proportional to the square of the amplitude of the input, while they were linear for transverse waves. Additionally, for small transverse impacts there was no perceptible longitudinal peak (figure 4*a*,*b*, red line), which may represent a way for webs to filter out small vibration sources that are less likely to contain biologically relevant information (e.g. gusts of wind) [12]. The observed nonlinearity would imply that, for larger amplitude impacts such as from prey, longitudinal wave amplitude will be more sensitive to changes in prey size than that of transverse waves. In theory, the ratio of transverse to longitudinal wave amplitude may provide a mechanism for estimating prey size and, if differential damping of transverse and longitudinal waves is taken into account [26], distance to the vibration source (time of arrival cannot be used to locate prey as the wavespeeds are too fast [17]). However, these mechanisms would be dependent on the spiders being able to separate transverse and longitudinal wave energy in their slit sensilla vibration receptors.

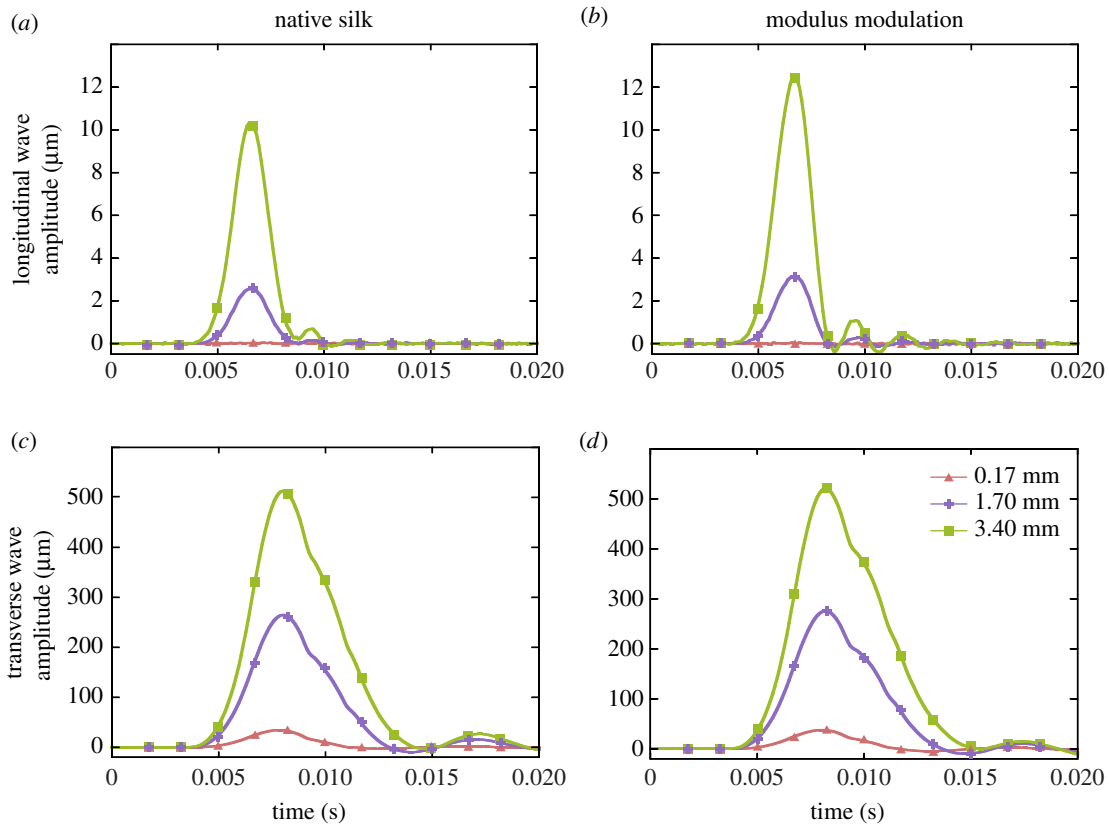

Figure 4. Nonlinearity in longitudinal waves. Amplitude–time data for longitudinal (*a*,*b*) and transverse (*c*,*d*) waves with 90° displacement input of 0.17 mm (red), 1.70 mm (blue) and 3.40 mm (green). Panels (*a*) and (*c*) use the average modulus value for native silk (11 GPa [5]), (*b*) and (*d*) use the minimum modulus value seen for major ampullate silk (4 GPa, after supercontraction [25]). (Online version in colour.)

In reality, very large amplitudes will lead to damping of vibrational energy as the radial threads yield, which was not accounted for in our models. Previously published modelling and experimental data suggest that internal damping can significantly damp vibrations by up to 50% when the silk stress is beyond the yield stress [40,41]. The relative importance of internal damping is an issue to be addressed in future work, for internal damping will be dependent on the loading history and hydration of the silk material, as well as the frequency and amplitude of vibration, and is likely to play different roles for transverse and longitudinal waves [40,42,43].

The FE models further showed that changing the modulus of the silk fibre does not affect maximum displacement amplitude for transverse waves, but increased the amplitude of longitudinal waves (figure 4). For transverse waves, the amplitude of the input was fixed by the solenoid, but for longitudinal waves a decrease in modulus decreased the wavespeed, which in turn increased the strain and so the amplitude.

A change of modulus is one outcome of supercontraction of major ampullate silk, which is also accompanied with a decrease in length and an increase in diameter [24,25,44]. For *A. diadematus* major ampullate silk, the maximum amount of supercontraction would lead to a change in modulus from 11 GPa to 4 GPa [25], as modelled in figure 4 (see electronic supplementary material, table S1), which is accompanied by a length shrinkage of 50% [25,45]. A change in modulus directly affects the speed of longitudinal waves [17], and figure 4 also suggests an effect of modulus change on longitudinal wave amplitude. Although not modelled here, a decrease in length and an increase in diameter should have no effect on longitudinal wave amplitude for a fixed magnitude transverse impact. Supercontraction will also affect transverse wave propagation, even though a change in modulus does not (figure 4*c*,*d*). Supercontraction has been shown to generate stresses of around 50 MPa when constrained [46–48] and this 'supercontraction stress' is thought to increase stress in radial threads following supercontraction to prevent sagging [45,47,49,50], which will increase the speed and amplitude of transverse waves (table 1).

The extent of dragline silk supercontraction is governed by silk tension. Supercontraction cannot occur at high fibre stresses above 140 MPa [24,51], so slack fibres can supercontract more as they do not have length restraints, and for non-slack fibres, low stress increases the amount of supercontraction. Therefore, radial threads may be more likely to supercontract when the web is slack, for example following impact of the web after the silk has yielded [52], which prevents transverse wave propagation.

We hypothesize that supercontraction of silk fibres is an important contributing factor to dragline silk wave propagation properties, as we know that it influences longitudinal and transverse wavespeeds and amplitudes via its effect on silk pre-stress and modulus [17]. This leads to the question of whether supercontraction could be important for web function, and if so whether supercontraction could be actively used by spiders to control web properties. Current hypotheses suggest that supercontraction has a role for silk tailoring [53] and web tightening [45,47,49,50]. We propose a hypothesis that bridges these theories, i.e. that supercontraction provides a control mechanism for the spider to balance mechanical and sensory functions. This novel hypothesis will be exciting to test and expand with further experimental data.

Theoretically, spiders could make use of supercontraction to control silk properties in two ways. Firstly, the extent of

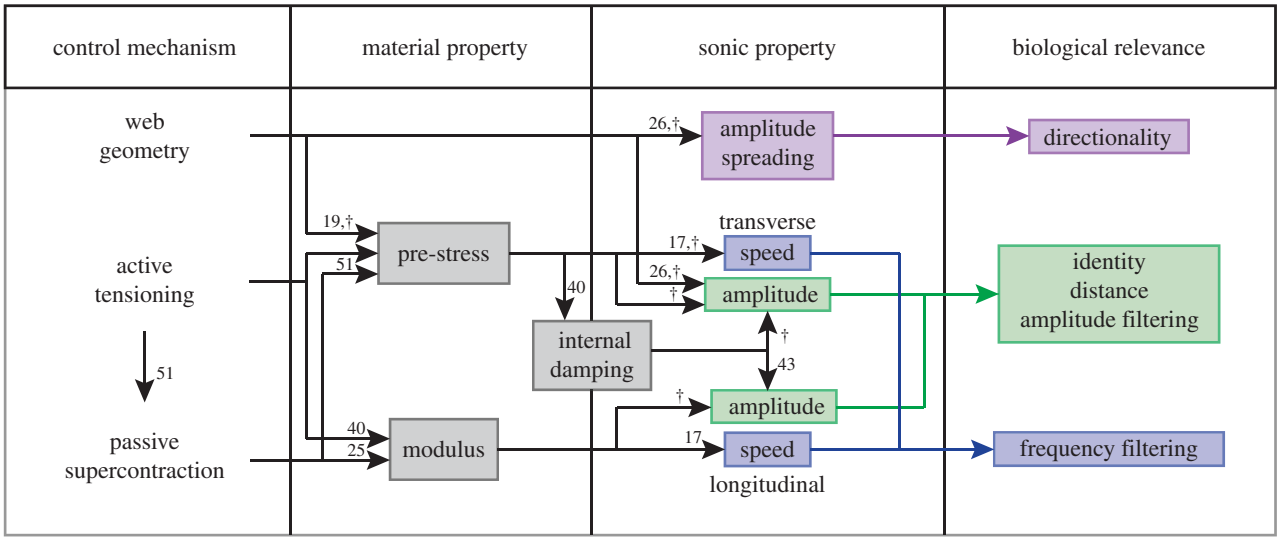

Figure 5. Linking available control mechanisms, silk properties and biological relevance. A reference is given for published data that support these links. † denotes that modelling or experimental evidence is given for this link in this manuscript. (Online version in colour.)

supercontraction in their webs could be controlled by actively altering radial thread tension during or after web building [18–20], as well as co-spinning minor ampullate silk during web building. Minor ampullate silk is often co-spun with major ampullate and does not supercontract [44], but its biological role in webs is still unclear [54,55]. It could have a role in controlling the extent of supercontraction of major ampullate threads, as minor ampullate is often seen to be 10% longer than their co-spun counterparts, which suggests that 'supercontraction stress' can also create slack in minor ampullate threads [50]. Practical use of controlling the extent of supercontraction by spiders is an open question, as factors such as weather conditions and web damage could also passively affect the extent of supercontraction via changes in humidity and web tension.

Secondly, spiders could make use of actively stretching supercontracted fibres to control silk modulus, pre-stress and length [17,51,53]. Subsequent stretching of supercontracted fibres by the spider in the hub after web building [20] would maintain fibre stresses at around 20% of the stress induced by the supercontraction process [48–50]. For example, in conditions where the web is slack from damage, supercontraction may be greater, which would increase pre-stress. Subsequent stretching can increase modulus to increase web stiffness, but reduce longitudinal wave amplitude, which may be desirable in certain conditions, e.g. higher wind where mechanical performance may be prioritized over sensory performance. Although both of these control mechanisms before and after supercontraction fit in with data on silk material properties, their utility by the spider in the web is a topic requiring further data.

The degree of supercontraction differs between spider species according to the proline content [25], but supercontraction stress appears to be unrelated to proline [51]. The degree of supercontraction between different spider clades shows some trends: Araneomorphae show higher levels of supercontraction, with highest levels in the Orbiculariae [51]. Correlations cannot be made to spider ecology in terms of wet versus dry climates [45], nor mode of prey capture (e.g. non-orb-weaving Orbiculariae also have high supercontraction levels; orb-weaving spiders from different families differ in supercontraction) [25,45,51]. Our hypothesis on the role of supercontraction for multifunctionality is supported by these phylogenetic observations, but further research is required to test whether supercontraction is more pronounced in clades that use major ampullate silks for both mechanical and sensory functions.

3.3. Linking silk properties, control and biological function

Orb webs are multifunctional structures that need to balance mechanical performance and information transfer to ensure that spiders can successfully catch prey, mate and avoid predators. Major ampullate silk is intrinsically multifunctional as it acts to absorb energy during web impact [2,52] and transmit vibrations to the spider [3,17]. Our data here showed that the capture spiral also has multiple functions; it not only acts to retain prey long enough for the spider to reach it, but is also an aspect of web architecture that directly affects transverse wave propagation. Although transverse waves dispersed to neighbouring radials via the capture spiral, longitudinal waves did not, which suggests that they could provide valuable information on the location of a vibration source.

We propose that two control mechanisms are available to the spider to allow it to adjust material properties and so cope with web multifunctionality: active tensioning of radial threads and supercontraction of major ampullate silk (figure 5), where both directly influence pre-stress and silk modulus [25,40,51,56]. Pre-stress and modulus control the sonic properties of the silk, including speed and amplitude of both transverse and longitudinal waves [17]. This is of direct utility to the spider. Wavespeed affects the frequency filtering of the web when wavelength is constrained, which amplify or damp vibrations according to their frequency. The relative amplitudes of transverse and longitudinal waves give information on vibration source identity (e.g. prey size) and distance, and the web also acts to filter out longitudinal waves from small impacts and transverse waves when pre-stress is zero (mostly likely post-impact). However, pre-stress and modulus also affect mechanical

performance, which represents a trade-off, but one that theoretically can be controlled by the spider.

Spiders, unlike most other animals are able to shape their immediate environment through making their own materials for integration into highly adapted structures. Spider behaviour and silk properties are variable but tunable, perhaps allowing spiders to shape their extended phenotype for multifunctional outcomes.

Data accessibility. Electronic supplementary material supporting this article is available through download. This includes Methods, Video S1, figures S1 and S2 and table S1.

Authors' contributions. B.M. conceived the research. B.M. and C.R.S. set-up the experimental procedure and Matlab analysis code. B.M. completed the experimental work and subsequent analysis. A.S. and R.Z. developed the web model, and A.S. set up the simulations and analysed the web model data. All authors contributed to data interpretation and article preparation.

Competing interests. We declare we have no competing interests.

Funding. For funding, we thank Jesus College, Oxford and the US Air Force Office of Scientific Research (FA9550-15-1-0264).

Acknowledgements. For loan of the PSV-400 vibrometer, we thank the EPSRC loan pool and the STFC staff at the Rutherford Appleton Laboratory. For his help with the spider husbandry, we thank Elliot Howard-Spink.

References

1. Foelix RF. 2010 *Biology of spiders*, 3rd edn. Oxford, NY: Oxford University Press.
2. Lin LH, Edmonds DT, Vollrath F. 1995 Structural engineering of an orb-spider's web. *Nature* **373**, 146–148. (doi:10.1038/373146a0)
3. Masters WM, Markl H. 1981 Vibration signal transmission in spider orb webs. *Science* **213**, 363–365. (doi:10.1126/science.213.4505.363)
4. Denny M. 1976 The physical properties of spider's silk and their role in design of orb-webs. *J. Exp. Biol.* **65**, 483–506.
5. Gosline JM, Guerette PA, Ortlepp CS, Savage KN. 1999 The mechanical design of spider silks: from fibroin sequence to mechanical function. *J. Exp. Biol.* **202**, 3295–3303.
6. Perry DJ, Bittencourt D, Siltberg-Liberles J, Rech EL, Lewis RV. 2010 Piriform spider silk sequences reveal unique repetitive elements. *Biomacromolecules* **11**, 3000–3006. (doi:10.1021/bm1007585)
7. Vollrath F, Edmonds DT. 1989 Modulation of the mechanical-properties of spider silk by coating with water. *Nature* **340**, 305–307. (doi:10.1038/340305a0)
8. Vollrath F, Edmonds D. 2013 Consequences of electrical conductivity in an orb spider's capture web. *Naturwissenschaften* **100**, 1163–1169. (doi:10.1007/s00114-013-1120-8)
9. Maklakov AA, Bilde T, Lubin Y. 2003 Vibratory courtship in a web-building spider: signalling quality or stimulating the female? *Anim. Behav.* **66**, 623–630. (doi:10.1006/anbe.2003.2245)
10. Suter RB. 1978 *Cyclosa turbinata* (Araneae, Araneidae)—prey discrimination via web-boune vibrations. *Behav. Ecol. Sociobiol.* **3**, 283–296. (doi:10.1007/bf00296314)
11. Vollrath F. 1979 Vibrations—their signal function for a spider kleptoparasite. *Science* **205**, 1149–1151. (doi:10.1126/science.205.4411.1149)
12. Masters WM. 1984 Vibrations in the orbwebs of *Nuctenea sclopetaria* (Araneidae). 2. Prey and wind signals and the spiders response threshold. *Behav. Ecol. Sociobiol.* **15**, 217–223. (doi:10.1007/bf00292978)
13. Tarsitano M, Jackson RR, Kirchner WH. 2000 Signals and signal choices made by the araneophagic jumping spider *Portia fimbriata* while hunting the orb-weaving web spiders *Zygiella x-notata* and *Zosis geniculatus*. *Ethology* **106**, 595–615. (doi:10.1046/j.1439-0310.2000.00570.x)
14. Barth FG. 1982 Spider vibration receptors—threshold curves of individual slits in the metatarsal lyriform organ. *J. Comp. Physiol.* **148**, 175–185. (doi:10.1007/BF00619124)
15. Liesenfeld FJ. 1961 Über leistung und sitz des erschütterungssinnes von netzspinnen. *Biol. Zbl.* **80**, 465–475.
16. Main IG. 1993 *Vibrations and waves in physics*, 3rd edn. Cambridge, UK: Cambridge University Press.
17. Mortimer B, Gordon SD, Siviour CR, Holland C, Vollrath F, Windmill JFC. 2014 The speed of sound in silk: linking material performance to biological function. *Adv. Mater.* **26**, 5179–5183. (doi:10.1002/adma.201401027)
18. Eberhard WG. 1981 Construction behaviour and the distribution of tensions in orb webs. *Bull. Br. Arachnol. Soc* **5**, 189–204.
19. Wirth E, Barth FG. 1992 Forces in the spider orb web. *J. Comp. Physiol. A* **171**, 359–371. (doi:10.1007/BF00223966)
20. Watanabe T. 2000 Web tuning of an orb-web spider, *Octonoba sybotides*, regulates prey-catching behaviour. *Proc. R. Soc. Lond. B* **267**, 565–569. (doi:10.1098/rspb.2000.1038)
21. Eberhard WG. 2013 The rare large prey hypothesis for orb web evolution: a critique. *J. Arachnol.* **41**, 76–80. (doi:10.1636/B12-34.1)
22. Liu Y, Shao ZZ, Vollrath F. 2005 Extended wet-spinning can modify spider silk properties. *Chem. Commun.* **19**, 2489–2491. (doi:10.1039/B500319A)
23. Vollrath F, Madsen B, Shao ZZ. 2001 The effect of spinning conditions on the mechanics of a spider's dragline silk. *Proc. R. Soc. Lond. B* **268**, 2339–2346. (doi:10.1098/rspb.2001.1590)
24. Guan J, Vollrath F, Porter D. 2011 Two mechanisms for supercontraction in *Nephila* spider dragline silk. *Biomacromolecules* **12**, 4030–4035. (doi:10.1021/bm201032v)
25. Liu Y, Sponner A, Porter D, Vollrath F. 2008 Proline and processing of spider silks. *Biomacromolecules* **9**, 116–121. (doi:10.1021/bm700877g)
26. Landolfa MA, Barth FG. 1996 Vibrations in the orb web of the spider *Nephila clavipes*: cues for discrimination and orientation. *J. Comp. Physiol. A* **179**, 493–508. (doi:10.1007/BF00192316)
27. Masters WM. 1984 Vibrations in the orbwebs of *Nuctenea sclopetaria* (Araneidae). 1. Transmission through the web. *Behav. Ecol. Sociobiol.* **15**, 207–215. (doi:10.1007/bf00292977)
28. Cranford SW, Tarakanova A, Pugno NM, Buehler MJ. 2012 Nonlinear material behaviour of spider silk yields robust webs. *Nature* **482**, 72–76. (doi:10.1038/nature10739)
29. Boutry C, Blackledge TA. 2009 Biomechanical variation of silk links spinning plasticity to spider web function. *Zoology* **112**, 451–460. (doi:10.1016/j.zool.2009.03.003)
30. Lin LH, Sobek W. 1998 Structural heirarchy in spider webs and spider web-type systems. *Struct. Eng.* **76**, 59–64.
31. Aoyanagi Y, Okumura K. 2010 Simple model for the mechanics of spider webs. *Phys. Rev. Lett.* **104**, 038102. (doi:10.1103/PhysRevLett.104.038102)
32. Tarakanova A, Buehler MJ. 2012 The role of capture spiral silk properties in the diversification of orb webs. *J. R. Soc. Interface* **9**, 3240–3248. (doi:10.1098/rsif.2012.0473)
33. Zaera R, Soler A, Teus J. 2014 Uncovering changes in spider orb-web topology owing to aerodynamic effects. *J. R. Soc. Interface* **11**, 20140484. (doi:10.1098/rsif.2014.0484)
34. Ko FK, Jovicic J. 2004 Modeling of mechanical properties and structural design of spider web. *Biomacromolecules* **5**, 780–785. (doi:10.1021/bm0345099)
35. Alam MS, Jenkins CH. 2005 Damage tolerance in naturally compliant structures. *Int. J. Damage Mech.* **14**, 365–384. (doi:10.1177/105678950504313)
36. Alam MS, Wahab MA, Jenkins CH. 2007 Mechanics in naturally compliant structures. *Mech. Mater.* **39**, 145–160. (doi:10.1016/j.mechmat.2006.04.005)
37. Craig CL. 1987 The ecological and evolutionary interdependence between web architecture and web silk spun by orb web weaving spiders. *Biol. J. Linn. Soc.* **30**, 135–162. (doi:10.1111/j.1095-8312.1987.tb00294.x)
38. Zemlin JC. 1968 *A study of the mechanical behavior of spider silks*. Technical Report 69-29-CM, AD 684333, US Army Natick Laboratories, Natick.

39. Drodge DR, Mortimer B, Holland C, Siviour CR. 2012 Ballistic impact to access the high-rate behaviour of individual silk fibres. *J. Mech. Phys. Solids* **60**, 1710–1721. (doi:10.1016/j.jmps.2012.06.007)
40. Guan J, Porter D, Vollrath F. 2012 Silks cope with stress by tuning their mechanical properties under load. *Polymer* **53**, 2717–2726. (doi:10.1016/j.polymer.2012.04.017)
41. Porter D, Guan J, Vollrath F. 2013 Spider silk: super material or thin fibre? *Adv. Mater*. **25**, 1275–1279. (doi:10.1002/adma.201204158)
42. Guan J, Porter D, Vollrath F. 2013 Thermally induced changes in dynamic mechanical properties of native silks. *Biomacromolecules* **14**, 930–937. (doi:10.1021/bm400012k)
43. Kolsky H. 1964 Stress waves in solids. *J. Sound Vib*. **1**, 88–110. (doi:10.1016/0022-460x(64)90008-2)
44. Work RW. 1977 Dimensions, birefringences, and force-elongation behavior of major and minor ampullate silk fibers from orb-web-spinning spiders—the effects of wetting on these properties. *Tex. Res. J*. **47**, 650–662.
45. Work RW. 1981 A comparative study of the supercontraction of major ampullate silk fibres of orb web building spiders (Araneae). *J. Arachnol*. **9**, 299–308.
46. Blackledge TA, Boutry C, Wong S-C, Baji A, Dhinojwala A, Sahni V, Agnarsson I. 2009 How super is supercontraction? Persistent versus cyclic responses to humidity in spider dragline silk. *J. Exp. Biol*. **212**, 1981–1989. (doi:10.1242/jeb.028944)
47. Guinea GV, Elices M, Perez-Rigueiro J, Plaza G. 2003 Self-tightening of spider silk fibers induced by moisture. *Polymer* **44**, 5785–5788. (doi:10.1016/s0032-3861(03)00625-6)
48. Savage KN, Guerette PA, Gosline JM. 2004 Supercontraction stress in spider webs. *Biomacromolecules* **5**, 675–679. (doi:10.1021/bm034270w)
49. Boutry C, Blackledge TA. 2013 Wet webs work better: humidity, supercontraction and the performance of spider orb webs. *J. Exp. Biol*. **216**, 3606–3610. (doi:10.1242/jeb.084236)
50. Work RW. 1985 Viscoelastic behavior and wet supercontraction of major ampullate silk fibers of certain orb-web-building spiders (Araneae). *J. Exp. Biol*. **118**, 379–404.
51. Boutry C, Blackledge TA. 2010 Evolution of supercontraction in spider silk: structure-function relationship from tarantulas to orb-weavers. *J. Exp. Biol*. **213**, 3505–3514. (doi:10.1242/jeb.046110)
52. Sensenig AT, Lorentz KA, Kelly SP, Blackledge TA. 2012 Spider orb webs rely on radial threads to absorb prey kinetic energy. *J. R. Soc. Interface* **9**, 1880–1891. (doi:10.1098/rsif.2011.0851)
53. Guinea GV, Elices M, Perez-Rigueiro J, Plaza GR. 2005 Stretching of supercontracted fibers: a link between spinning and the variability of spider silk. *J. Exp. Biol*. **208**, 25–30. (doi:10.1242/jeb.01344)
54. Guinea GV *et al.* 2012 Minor ampullate silks from *Nephila* and *Argiope* spiders: tensile properties and microstructural characterization. *Biomacromolecules* **13**, 2087–2098. (doi:10.1021/bm3004644)
55. Hesselberg T, Vollrath F. 2012 The mechanical properties of the non-sticky spiral in *Nephila* orb webs (Araneae, Nephilidae). *J. Exp. Biol*. **215**, 3362–3369. (doi:10.1242/jeb.068890)
56. Liu Y, Shao ZZ, Vollrath F. 2008 Elasticity of spider silks. *Biomacromolecules* **9**, 1782–1786. (doi:10.1021/bm7014174)